

Results

NM reduced in situ 26S proteasome activity in SH-SY5Y cells

After treatment with NM, the accumulation of ZsGFP was observed in cytoplasm by fluorescence microscopy (Fig. 1A). The increased ZsGFP fluorescence in the cells was quantified in a RF-5300 spectrophotofluorometer. As shown in Fig. 1B, the fluorescence intensity increased in a dose- and time-dependent way. The ZsGFP fluorescence increased in the cells treated with 0.05 and 0.1 $\mu\text{g/ml}$ of NM and further increased after 3 days' incubation in the presence of 0.1 $\mu\text{g/ml}$ NM. NM at these concentrations neither affected cell proliferation, nor induced morphological changes in SH-SY5Y cells.

NM directly inhibited in vitro ubiquitin-26S proteasome activity

The direct effect of NM on ubiquitin-26S proteasome activity was examined using the enzyme samples prepared from SH-SY5Y cells, and ubiquitinated

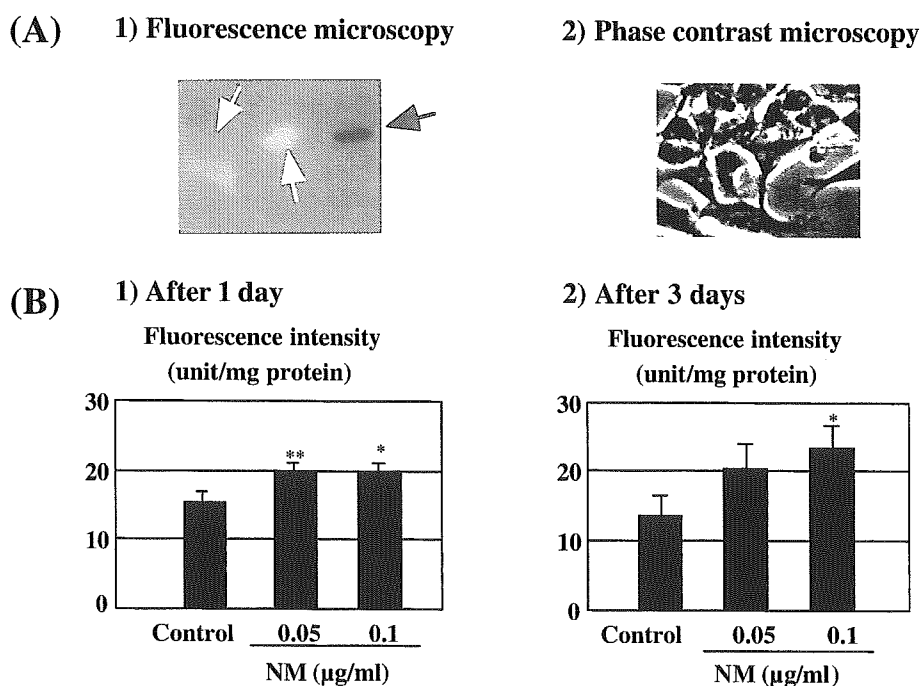
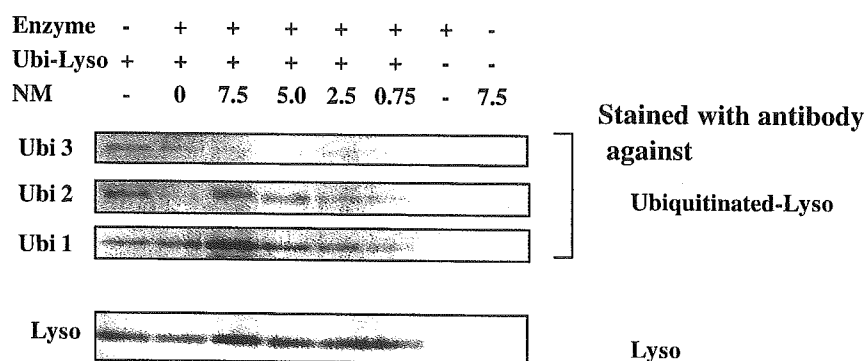


Fig. 1. Effects of neuromelanin (NM) on the *in situ* activity of 26S proteasome in SH-SY5Y cells transfected with the proteasome sensor vector (PSV-SH-SY5Y cells). **A** Morphological observation of PSV-SH-SY5Y cells treated with NM. The cells were cultured in the presence of 0.1 $\mu\text{g/ml}$ of NM for 3 days and accumulation of ZsGFP (white arrows) and NM (black arrow) was observed by fluorescence microscopy (1) and phase contrast microscopy (2). **B** Quantitation of ZsGFP fluorescence in PSV-SH-SY5Y cells treated with 0.05 and 0.1 $\mu\text{g/ml}$ of NM for 1 to 3 days. The fluorescence intensity was quantified using a fluorospectrophotometer with excitation at 493 nm and emission at 505 nm, and expressed as arbitrary fluorescence unit/mg protein. The column and bar represent mean and SD of 3 experiments. After the treatment with NM, the fluorescence intensity increased in a dose- and time-dependent manner compared to Control treated with L-Cyst-DMSO solution. * $p < 0.05$ and ** $p < 0.01$ by ANOVA compared to Control

(A)



(B)

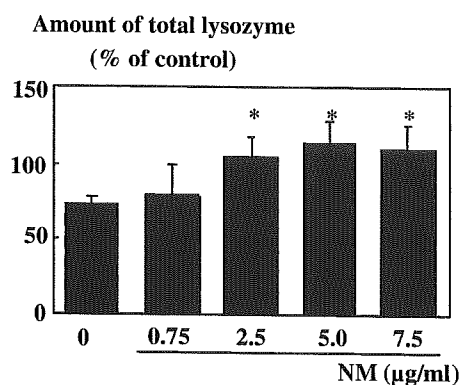


Fig. 2. Effects of neuromelanin (NM) on the *in vitro* activity of 26S proteasome. **A** The effects of NM on the activity measured with polyubiquitinated lysozyme (Lyso), a specific substrate for 26S proteasome. Mono-, di- and tri-ubiquitinated Lyso (Ubi 1, Ubi 2, Ubi 3), was prepared as described in the Materials and methods. Western blotting shows the degradation of ubiquitinated (Ubi) and non-ubiquitinated free Lyso after incubation with the enzyme preparation pre-treated with L-Cyst-DMSO solution in the absence or presence of NM. Ubiquitinated Lyso (Ubi 1, Ubi 2 and Ubi 3) was visualized with anti-polyubiquitinated antibody, and Lyso with anti-Lyso antibody. NM treatment reduced the degradation of ubiquitinated Lyso, especially Ubi 2 and Ubi 3, significantly. **B** The effect of NM on the total amount of Lyso (ubiquitinated and free). The amounts were quantified by measuring proteins stained with anti-Lyso antibody and using NIH imaging as described in the Materials and methods. The column and bar represent mean and SD of 3 independent experiments. NM significantly inhibited the ubiquitin-26S proteasome dependent degradation of Lyso significantly. * $p < 0.05$ by ANOVA compared to control treated by L-Cyst-DMSO solution without NM (0)

Lyso as a substrate specific for 26S proteasome. Figure 2A shows the immunoblotting of mono-, di- and tri-ubiquitinated Lyso and non-ubiquitinated Lyso. In the enzyme preparation and the NM suspension, ubiquitinated proteins were not detected. After 4 h incubation with the enzyme preparation, the amounts of ubiquitinated Lyso, especially di- and tri-ubiquitinated Lyso, were decreased significantly. In this system the ubiquitin ligase activity was not inhibited, and the amount of Lyso itself decreased. The total amounts of Lyso (free and ubiquitinated) were increased with NM, indicating that NM inhibited the Lyso

degradation by ubiquitin-26S proteasome system (Fig. 2B). The inhibition was increased by NM from 0.75 to 2.5 $\mu\text{g}/\text{ml}$, and reached to a plateau, indicating the soluble NM might be saturated.

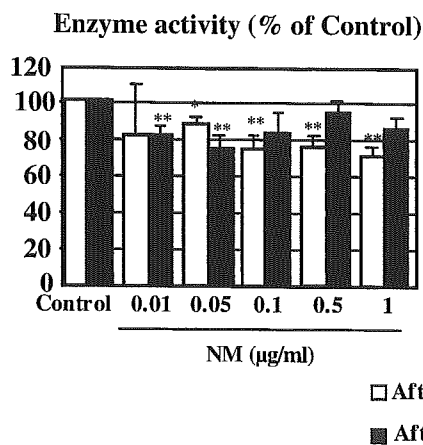
Effects of NM on proteasome activities in cells

In the cells treated with NM for 1–3 days, the proteasome activities were measured using synthetic substrates, LLVY-MCA for chymotrypsin-like activity or LLE-MCA for peptidyl-glutamyl peptide hydrolase-like activity without addition of ATP. The activity represented mainly that of 20S proteasome, but the contribution of 26S could not be completely excluded. As shown in Fig. 3, the catalytic activity towards LLVY-MCA and LLE-MCA reduced after the incubation with NM, but the inhibition was not so marked. Reduction of the activity was more prominent in the cells treated with NM for 1 day, and after 3 days the reduced activity tended to be restored.

NM did not inhibit in vitro 20S proteasome activity directly

The proteasome activity in the enzyme preparation from control SH-SY5Y cells was measured with the synthetic substrates without addition of ATP. NM at the concentrations up to 7.5 $\mu\text{g}/\text{ml}$ in the reaction mixture did not inhibit the enzyme activity *in vitro*, as shown in Fig. 4.

(A) Chymotrypsin-like



(B) Peptidyl-glutamyl peptide hydrolase-like

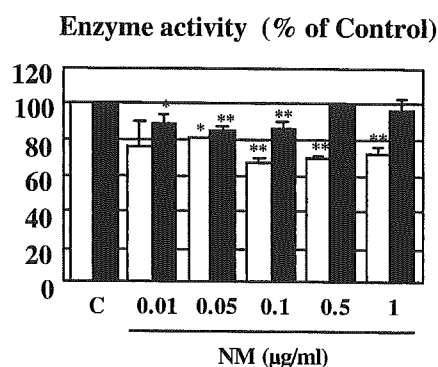
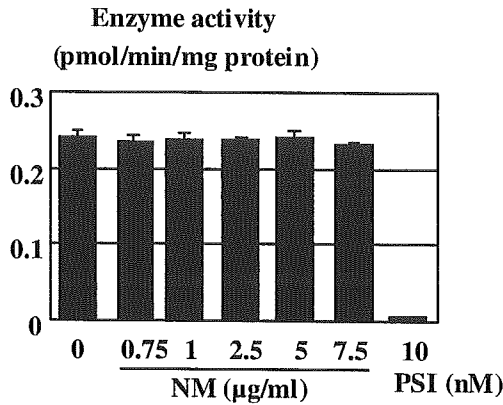


Fig. 3. Effects of neuromelanin (NM) on the proteasome activities in the cells treated with NM. The cells were cultured with L-Cyst-DMSO solution in the absence (Control) or presence of 0.01–1 $\mu\text{g}/\text{ml}$ of NM for 1 and 3 days, then the enzyme sample was prepared. The chymotrypsin-like (A) and peptidyl-glutamyl peptide hydrolase-like (B) proteasome activities were measured with synthetic substrates. The column and bar represent mean and SD of 3 independent experiments. The activity was expressed as percent of Control. Open column and filled column; the proteasome activity in the cells after 1 day and 3 days treatment with NM, respectively. * $p < 0.05$ and ** $p < 0.01$ by ANOVA compared to control without NM treatment (C)

(A) Chymotrypsin-like



(B) Peptidyl-glutamyl peptide hydrolase-like

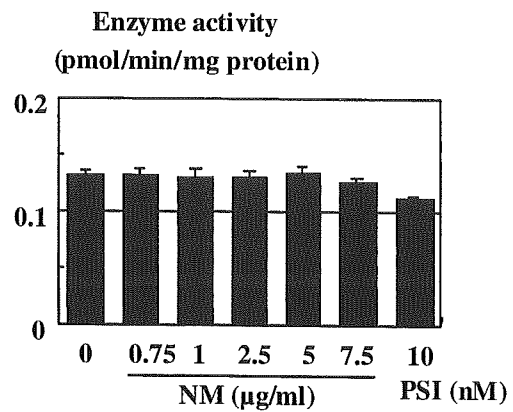


Fig. 4. Effects of neuromelanin (NM) on *in vitro* activities of chymotrypsin-like or peptidyl-glutamyl peptide hydrolase-like proteasome. The activities in the enzyme preparation were measured in the absence and presence of NM (0.75–7.5 µg/ml at the final concentrations), using artificial substrates, as described in Materials and Methods. The enzyme activity was expressed as pmole AMC produced/min/mg protein. The column and bar represent mean and SD of 4 independent experiments. NM did not reduce the chymotrypsin-like (A) or peptidyl-glutamyl peptide hydrolase-like (B) activity, but a proteasome inhibitor, PSI (10 nM) inhibited chymotrypsin-like proteasome activity completely

(A) After 1 day

(B) After 3 days

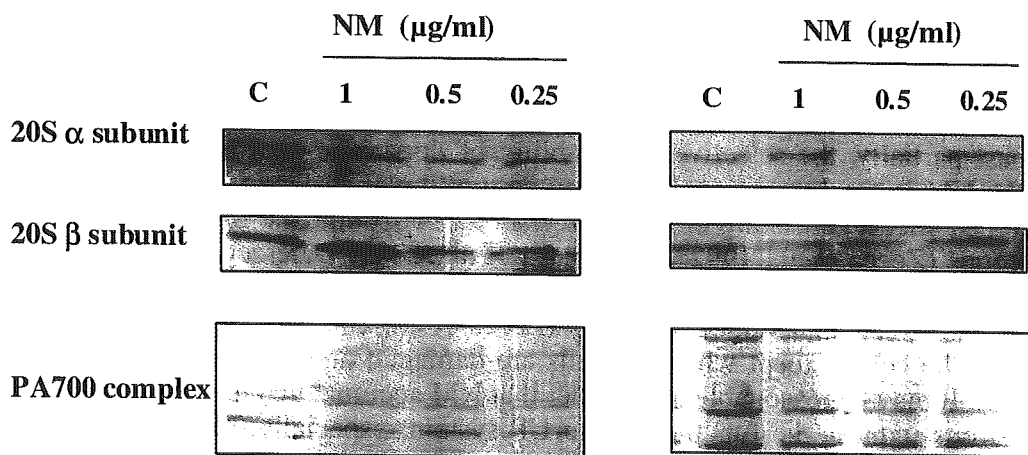


Fig. 5. Effect of neuromelanin (NM) on the protein levels of α- and β-subunits of 20S proteasome and PA700 complex of 26S proteasome. The cells were incubated with L-Cyst-DMSO solution in the absence or presence of NM (0.25–1 µg/ml) for 1 and 3 days and the cell lysate was subjected to Western blot analysis, using antibody against 20S α- and β-subunits and PA700 complex, respectively. NM reduced the level of PA700 complex, but did not affect the level of 20S α- and β-subunits in SH-SY5Y cells after 3 days' culture

*NM reduced the protein level of PA700 complex, but not 20S
 α - and β -subunit*

To examine the effect of NM on the protein levels of proteasome subunits, proteins in the cells treated with NM at 0.25–1 $\mu\text{g}/\text{ml}$ for 1–3 days were analyzed using polyclonal antibodies against α - and β -subunits of 20S proteasome, and a proteasome activator PA700 complex. As shown in Fig. 5, the protein level of PA700 complex was reduced significantly after 3 days of treatment, whereas NM did not affect the protein levels of α and β subunits of 20S under the conditions examined.

Discussion

The results presented here clearly demonstrate that NM inhibits 26S proteasome activity *in situ* and *in vitro* whereas it did not inhibit the *in vitro* activity of 20S proteasome, nor reduced the protein levels of 20S α - and β -subunit in SH-SY5Y cells. NM treatment reduced the *in vitro* activity of 26S proteasome measured by use of ubiquitinated Lyso as a substrate, which was confirmed further by the increased fluorescence of the proteasome sensor protein, ZsGFP. In addition, NM reduced ubiquitination of free Lyso by E1, E2 and E3 ligase *in vitro* as shown by increased level of free Lyso in the reaction mixture. The inhibition of ubiquitin-26S proteasome system by NM may be due to the direct inhibition of the enzyme activities, by binding of soluble NM components to the active sites. In addition, NM reduced the protein level of a proteasome activator, PA700 complex, which forms active 26S proteasome by binding to the 20S proteasome and makes it possible to degrade polyubiquitinated proteins. The result presented here may be relevant to the recent report that the levels of the PA700 subunit and α -subunit of 20S proteasome were significantly reduced in the SN of PD brains (McNaught et al., 2003). However, the detailed molecular mechanism underlying the reduction of 26S proteasome activity by NM remains to be clarified.

The involvement of NM in impaired function of UP system may explain, at least partially, the selective vulnerability of dopamine neurons in ageing and PD. NM is a polymeric molecule having multilayer structure with planar overlapped sheets consisting of dihydroxyindole, benzothiazine rings and aliphatic groups (Zecca et al., 1992; Wakamatsu et al., 2003; Dzierzega-Lecznar et al., 2004). NM accumulates continuously in dopamine neurons of SN during aging reaching very high values in elderly (Zecca et al., 2002), and it is not secreted from the cells, except when the cells are damaged and phagocytosed by glial cells. It may be reasonable to consider that NM accumulated in nigral dopamine neurons reduces the function of the UP system, especially 26S and increases accumulation of ubiquitinated and denatured proteins. Indeed, Lewy bodies were found in the SN in subjects who had no Parkinsonian symptoms or signs during life and were suggested that this "Incidental Lewy body" represents early, subclinical PD (Forno and Langston, 1993). In normal ageing the accumulation of NM does not cause neuronal degeneration probably because some agents block the interaction between NM and proteasome however in PD it is possible that these blocking molecules are removed or not expressed, therefore

NM could inhibit proteasome and trigger the cascade ending into neuronal death.

Under the conditions used in this study, NM treatment did not induce the cell death in SH-SY5Y cells, indicating that other factors may be involved in the final cell death. The mitochondrial dysfunction, and reduction of ATP synthesis may further enhance the inhibition of the UP activity in dopamine neurons, since the activity of 26S, but not 20S, depends on ATP level. Recently we found that mitochondrial dysfunction caused by rotenone, a complex I inhibitor, increased modification of the 20S proteasome subunit with acrolein, and reduced the activity of proteasome, through binding of aggregated oxidized protein to the catalytic site (Shamoto-Nagai et al., 2003). These results suggest that the mitochondrial dysfunction, increased oxidative stress and impairment of the UP system may interact with each other, resulting in the cell death of dopamine neurons in ageing and PD.

The induction of cell death by accumulated modified protein may be due to occupation of limited space in cells, change in the signal transduction, or by inhibition of transcription of important genes, but it requires further studies for full elucidation. In addition, it is not clear whether NM itself or NM components, including quinones, products of dopamine, oxidized products of lipid and protein, or trace metals was truly cytotoxic and inhibited proteasome activity. Further molecular studies will elucidate full mechanistic features of the involvement of NM in degeneration of dopamine neurons in the brain.

Acknowledgements

We thank to Ms. H. Nishitani and Y. Yamaoka for their skilful assistance during this study. This work was supported by a Grant-in-Aid on Scientific Research (C) (W. M.) and (A) (W. M. and T. O.), and for Scientific Research (Y. A, No. 09670859), from Japan Society for the Promotion of Science, Grant for Clinical Research for Evidence Based Medicine (W. M., M. N., Y. A.) from the Ministry of Health, Labor and Welfare, Japan. F. T. was supported by the PhD stipend DOC awarded by the Austrian Academy of Sciences. F. T. and P. R. were supported by the National Parkinson Foundation, Miami, Florida, USA. F. A. Z. and L. Z. acknowledge the support of FIRB-Ministry of Science, Italy. We would like to thank Dr. Th. Arzberger for providing help in preparing the tissue.

References

- BenShachar D, Riederer P, Youdim MB (1991) Iron-melanin interaction and lipid peroxidation: implications for Parkinson's disease. *J Neurochem* 62: 369–371
- Bradford MM (1976) A rapid and sensitive method for quantitation of microgram quantities of protein using the principle of protein dye binding. *Anal Biochem* 72: 248–254
- D'Amato RJ, Lipman ZP, Snyder SH (1986) Selectivity of the Parkinson neurotoxin, MPTP: toxic metabolite MPP⁺ binds to neuromelanin. *Science* 231: 987–989
- Double KL, Ben-Schachar D, Youdim MB, Zecca L, Riederer P, Gerlach M (2002) Influence of neuromelanin on oxidative pathway within the human substantia nigra. *Neurotoxicol Teratol* 24: 621–628
- Double KL, Gerlach M, Schünemann V, Trautwein AX, Zecca L, Gallorini M, Youdim MBH, Riederer P, Ben-Shachar D (2003) Iron binding characteristics of neuromelanin of the human substantia nigra. *Biochem Pharmacol* 66: 489–494
- Dzierzega-Leczna A, Kurkiewicz S, Stepien K, Chodurek E, Wilczok T, Arzberger T, Riederer P, Gerlach M (2004) GC/MS analysis of thermally degraded neuromelanin from the human substantia nigra. *J Am Soc Mass Spect* 15: 920–926

- Emborg ME, Ma SY, Mufson EJ, Levey AI, Taylor MD, Brown WD, Holden JE, Korgower JH (1998) Age-related declines in nigral neuronal function correlate with motor impairments in rhesus monkeys. *J Comp Neurol* 16: 253–265
- Forno LS, Langston JW (1993) Lewy bodies and ageing: relation to Alzheimer's and Parkinson's disease. *Neurodegeneration* 2: 19–24
- Gai WP, Yuan HX, Li XQ, Power JT, Blumbergs PC, Jensen PH (2000) In situ and in vitro study of colocalization and segregation of α -synuclein, ubiquitin, and lipids in Lewy bodies. *Exp Neurol* 166: 324–333
- Gerlach M, Trautwein AX, Zecca L, Youdim MB, Riederer P (1995) Mossbauer spectroscopic studies of purified human neuromelanin isolated from the substantia nigra. *J Neurochem* 65: 923–926
- Hirsch E, Graybiel AM, Agid YA (1988) Melanized dopaminergic neurons are differentially susceptible to degeneration in Parkinson's disease. *Nature* 334: 345–348
- Ii K, Ito H, Tanaka K, Hirano A (1997) Immunochemical co-localization of the proteasome in ubiquitinated structures in neurodegenerative diseases and the elderly. *J Neuropathol Exp Neurol* 56: 125–131
- Jellinger K, Kienzl E, Rumpelmair G, Riederer P, Stachelberger H, Ben-Shachar D, Youdim MB (1992) Iron-melanin complex in substantia nigra of parkinsonian brains: an x-ray microanalysis. *J Neurochem* 59: 1168–1171
- Kastner A, Hirsch EC, Lejeune O, Javoy-Agid F, Rascol O, Agid Y (1992) Is the vulnerability of neurons in the substantia nigra of patients with Parkinson's disease related to their neuromelanin contents? *J Neurochem* 59: 1080–1089
- Kitada T, Asakawa S, Hattori N, Matsumine H, Yamamura Y, Minoshima S, Yokochi M, Mizuno Y, Shimizu N (1998) Mutations in the parkin gene cause autosomal recessive juvenile parkinsonism. *Nature* 392: 605–608
- Leroy E, Boyer R, Auburger G, Leube B, Ulm G, Mezey E, Harta G, Brownstein MJ, Jonnalagada S, Chernova T, Dehejia A, Lavedan C, Gasser T, Steinbach PJ, Wilkinson KD, Polymeropoulos MH (1998) The ubiquitin pathway in Parkinson's disease. *Nature* 395: 451–452
- Linquist NG, Larsson BS, Lyden-Sokolowski A (1987) Neuromelanin and its possible protective and destructive properties. *Pigment Cell Res* 1: 133–136
- Mann DMA, Yates PO (1979) The effects of aging on the pigmented nerve cells of the human locus coeruleus and substantia nigra. *Acta Neuropathol* 47: 93–97
- Maruyama W, Boulton AA, Davis BA, Dostert P, Naoi M (2001) Enantio-specific induction of apoptosis by an endogenous neurotoxin, N-methyl(R)salsolinol, in dopaminergic SH-SY5Y cells: suppression of apoptosis by N-(2-heptyl)-N-methylpropargylamine. *J Neural Transm* 108: 11–24
- McNaught KS, Bjorklund LM, Belizaire R, Isacson O, Jenner P, Olanow CW (2002a) Proteasome inhibition causes nigral degeneration with inclusion bodies in rats. *Neuroreport* 13: 1437–1441
- McNaught KS, Shashidharan P, Perl DP, Jenner P, Olanow CW (2002b) Aggresome-related biogenesis of Lewy bodies. *Eur J Neurosci* 16: 2136–2148
- McNaught KS, Belizaire R, Isacson O, Jenner P, Olanow CW (2003) Altered proteasomal function in sporadic Parkinson's disease. *Exp Neurol* 179: 38–46
- Mochizuki H, Nishi K, Mizuno Y (1993) Iron-melanin complex is toxic to dopaminergic neurons in a nigrostriatal co-culture. *Neurodegeneration* 2: 1–7
- Naoi M, Maruyama W, Dostert P (1994) Binding of 1,2(N)-dimethyl-6,7-dihydroxy-isoquinolinium ion to melanin: effects of ferrous and ferric ion on the binding. *Neurosci Lett* 171: 9–12
- Oestergren A, Annas A, Skog K, Lindquist NG, Brittebo EB (2004) Long-term retention of neurotoxic beta-carbolines in brain neuromelanin. *J Neural Transm* 111: 141–157
- Offen D, Ziv I, Gorodin S, Glater E, Hochman A, Melamed E (1997) Dopamine-melanin induces apoptosis in PC12 cells; possible implications for the etiology of Parkinson's disease. *Neurochem Int* 141: 32–39
- Okada K, Wangpoengtrakul C, Osawa T, Toyokuni S, Tanaka K, Uchida K (1999) 4-Hydroxy-2-nonenal-mediated impairment of intracellular proteolysis during oxidative stress. *J Biol Chem* 272: 23787–23793

- Polymeropoulos MH, Lavedan C, Leroy E, Ide SE, Dehejia A, Dutra A, Pike B, Root H, Rubenstein J, Boyer R, Stenroos ES, Chandrasekharappa S, Athanassiadou A, Papapetropoulos T, Johnson WG, Lazzarini AM, Duvoisin RC, Di Iorio G, Golbe LI, Nussbaum RL (1997) Mutation in the α -synuclein gene identified in families with Parkinson's disease. *Science* 276: 2045–2047
- Rodgers KJ, Dean RT (2003) Assessment of proteasome activity in cell lysates and tissue homogenates using peptide substrates. *Int J Biochem Cell Biol* 35: 716–727
- Shamoto-Nagai M, Maruyama W, Kato Y, Isobe K, Tanaka M, Naoi M, Osawa T (2003) An inhibitor of mitochondrial complex I, rotenone, inactivates proteasome by oxidative modification and induced aggregation of oxidized proteins in SH-SY5Y cells. *J Neurosci Res* 74: 589–597
- Shimura H, Hattori N, Kubo S, Mizuno Y, Asakawa S, Minoshima S, Shimizu N, Iwai K, Chiba T, Tanaka K, Suzuki T (2000) Familial Parkinson's disease gene product, parkin, is a ubiquitin-protein ligase. *Nat Genet* 25: 302–305
- Shimura H, Schlossmacher MG, Hattori N, Prosch MP, Trockenbacher A, Schneider R, Mizuno Y, Kosik KS, Selkoe DJ (2001) Ubiquitination of a new form of α -synuclein by parkin from human brain: implications for Parkinson's disease. *Science* 293: 263–269
- Shringarpure R, Grune T, Mehlhase J, Davis KJ (2003) Ubiquitin-conjugation is not required for the degradation of oxidized proteins by proteasome. *J Biol Chem* 278: 311–318
- Sulzer D, Bogulavsky J, Larsen KE, Behr G, Karatekin E, Kleinman MH, Turro N, Krantz D, Edwards RH, Greene LA, Zecca L (2000) Neuromelanin biosynthesis is driven by excess cytosolic catecholamines not accumulated by synaptic vesicles. *Proc Natl Acad Sci USA* 97: 11869–11974
- Wakamatsu K, Fujikawa K, Zucca FA, Zecca L, Ito S (2003) The structure of neuromelanin as studied by chemical degradative methods. *J Neurochem* 86: 1015–1023
- Wilms H, Rosenstiel P, Sievers J, Deuschl G, Zecca L, Lucius R (2003) Activation of microglia by human neuromelanin is NF- κ B-dependent and involves p38 mitogen-activated protein kinase: implications for Parkinson's disease. *FASEB J* 17: 500–502
- Youdim MB, Ben-Shachar D, Riederer P (1994) The enigma of neuromelanin in Parkinson's disease substantia nigra. *J Neural Transm (Suppl)* 43: 113–122
- Zareba M, Bober A, Korytowski W, Zecca L, Sarna T (1995) The effect of a synthetic neuromelanin on yield of free hydroxyl radicals generated in model systems. *Biochim Biophys Acta* 1271: 343–348
- Zecca L, Pietra R, Goj C, Mecacci C, Radice D, Sabbioni E (1994) Iron and other metals in neuromelanin, substantia nigra and putamen of human brain. *J Neurochem* 62: 1097–1101
- Zecca L, Shima T, Stroppolo A, Goj C, Battiston GA, Gerbasi R, Sarna T, Swartz HM (1996) Interaction of neuromelanin and iron in substantia nigra and other areas of human brain. *Neuroscience* 73: 407–415
- Zecca L, Costi P, Mecacci C, Ito S, Terreni M, Sonnino S (2000) Interaction of human substantia nigra neuromelanin with lipids and peptides. *J Neurochem* 74: 1758–1765
- Zecca L, Fariello R, Riederer P, Sulzer D, Gatti A, Tampellini D (2002) The absolute concentration of nigral neuromelanin, assayed by a new sensitive method, increases throughout the life and is dramatically decreased in Parkinson's disease. *FEBS Lett* 510: 216–220

Authors' address: Dr. W. Maruyama, Section of Biochemistry, Department of Mechanism of Ageing, National Center for Geriatrics and Gerontology, Morioka-cho, Obu, Aichi 474-8522, Japan, e-mail: maruyama@nils.go.jp



A highly bioactive lignophenol derivative from bamboo lignin exhibits a potent activity to suppress apoptosis induced by oxidative stress in human neuroblastoma SH-SY5Y cells

Yukihiro Akao,^{a,*} Norio Seki,^b Yoshihito Nakagawa,^a Hong Yi,^a Kenji Matsumoto,^a Yukie Ito,^c Kuniyasu Ito,^b Masamitsu Funaoka,^d Wakako Maruyama,^e Makoto Naoi^a and Yoshinori Nozawa^a

^aGifu International Institute of Biotechnology, Kakamigahara, Gifu 504-0838, Japan

^bGifu Prefectural Human Life Technology Research Institute, Takayama, Gifu 506-0058, Japan

^cAichi-Konan college, Konan, Aichi 483-8086, Japan

^dFaculty of Bioresources, Mie University, Tsu, Mie 514-8507, Japan

^eNational Institute of Longevity Sciences, Obu, Aichi 474-8522, Japan

Received 13 May 2004; revised 9 July 2004; accepted 9 July 2004

Available online 6 August 2004

Abstract—Approaches to protection against neurodegenerative diseases, in which oxidative stress and inflammation are implicated, should be based on the current concept on the etiology of these diseases. Recently, a new therapeutic strategy has been proposed to protect neurons from cell death by attenuating the apoptotic signal transduction. Lignin, a durable aromatic network polymer second to cellulose in abundance, was able to be converted into highly active lignophenol derivatives with antioxidant activity by using our newly developed phase-separation technique. These lignophenol derivatives were found to show the potent neuroprotective activity against oxidative stress. Among the compounds examined, a lignocresol derivative from bamboo (lig-8) exhibited the most potent neuroprotective activity against hydrogen peroxide (H₂O₂)-induced apoptosis in human neuroblastoma cell line SH-SY5Y by preventing the caspase-3 activation via either caspase-8 or caspase-9. Furthermore, it was found that lig-8 exerted the antiapoptotic effect by inhibiting dissipation of the mitochondrial membrane permeability transition induced by H₂O₂ or by the peripheral benzodiazepin receptor ligand PK11195. Lig-8 was also shown to be potent in the antioxidant activity in the cells exposed to H₂O₂, as assessed by flow cytometry using 5-(and-6)-chloromethyl-2',7'-dichlorodihydrofluorescein diacetate and in vitro reactive oxygen species-scavenging potency. These data suggest that lig-8 is a promising neuroprotector, which affects the signaling pathway of neuronal cell death and that it would be of benefit to delay the progress of neurodegenerative diseases.

© 2004 Elsevier Ltd. All rights reserved.

1. Introduction

The plant cell wall is a complicated semi-interpenetrating network structure built up from cellulose, hemicellulose, and lignin. Lignin is a durable aromatic network polymer second to cellulose in natural abundance. However, the utilization of lignin has not yet been successfully achieved, because lignin molecules lack stereoregularity and also the repeating units in the molecule are heterogeneous and complex. In addition, ligno-

cellulosics components cannot be separated by the simple extraction processes because of nonselective modifications during the drastic isolation process such as the pulping processes, which make lignin molecules even more heterogeneous.

Recently, a new phase-separation system for production of functional lignin derivatives from native lignins was devised.^{1,2} This system utilizes phenols and concentrated acid. The resulting lignin derivatives, lignophenols, have highly phenolic function, high stability, and less heterogeneous compared with those after the conventional lignin preparations. The phenolic properties of lignophenols can be modulated by using different phenols.³ Thus, it can be assumed that the lignophenols derived

Keywords: Lignophenols; Antioxidant; Oxidative stress; Neuronal cell death; Neuroprotection.

* Corresponding author. Tel.: +81-583-71-4646; fax: +81-583-71-4412; e-mail: yakao@giib.or.jp

from native lignins have different phenolic functionalities to exhibit various biological activities. Moreover, the functionality of lignophenols is able to be easily modulated by various modifications.⁴

The antihuman immunodeficiency virus activity of lignins such as lignosulfonate isolated by pulping processes⁵ and lignin-like substance extracted from lignocellulosics,⁶ and anticancer activity of lignin F⁷ have been previously reported. However, these lignins can hardly be used as medicinal resources, because they cannot be mass-produced practically and their molecules are highly heterogeneous.

Apoptosis is an active, energy-dependent process through which living cells initiate their own death, and it is induced by a variety of physiological and pharmacological stimuli. Some clinical evidences show that disturbed apoptotic cell death is associated with certain diseases, such as cancers and immuno-insufficiencies. On the other hand, apoptosis is now considered to be the major death mode of neurons in neurodegenerative disorders such as Parkinson's disease (PD), Alzheimer's disease, and Huntington's disease.⁸ In PD, apoptotic features of dopaminergic neurons were detected in the substantia nigra of brains by the terminal deoxynucleotidyl transferase-mediated nick end labeling method or by electromicroscopic study.⁹

Previous studies have indicated that the neuronal toxicity is mediated and enhanced by reactive oxygen species (ROS) or reactive nitrogen species (RNS) and thus that the oxidative stress accelerates the cell death of neuronal cells in neurodegenerative disorders.^{10,11} In fact, such neuronal cell death has been reported to be attenuated by antioxidants and free radical scavengers.^{12,13} Recent

studies have shown that green tea polyphenols reduced free radical-induced lipid peroxidation.¹² Tea polyphenols have been attracting increasing interest because of their antioxidant, anti-inflammatory,^{14,15} anticarcinogenic,^{16,17} and iron chelating properties,¹⁸ as demonstrated both in vivo and in vitro. In addition to such properties, these compounds can penetrate the blood-brain barrier,¹⁹ and so may be promising for the development of drugs for treatment or prevention of neurodegenerative diseases associated with oxidative stress. In the present study, we have demonstrated the preventive effect of a highly bioactive lignophenol on the cell death induced by oxidative stress, and also showed that its neuroprotective activity was due to inhibition of caspase activation, prevention of dissipation of the mitochondrial membrane permeability transition (PT), and ROS- or RNS-scavenging activity.

2. Results and discussion

2.1. Characteristics of lignophenol derivatives

Native lignins with complicated 3-dimensional structures were converted to lignophenols by the phase-separation system, the summary of which is given in Figure 1. Lignophenols retain the original interunit linkages formed by dehydrogenative polymerization during the biosynthesis of native lignin, and have high phenolic functionality. By using different phenols for the phase-separation system, the different kinds of lignophenols were produced. Lignopolyphenols, such as lignocatechol, lignoresorcinol, and lignopyrogallol, which have many phenolic hydroxyl groups, are highly hydrophilic. On the other hand, lignomonophenols combined with monohydric phenols such as cresol are water-insoluble.

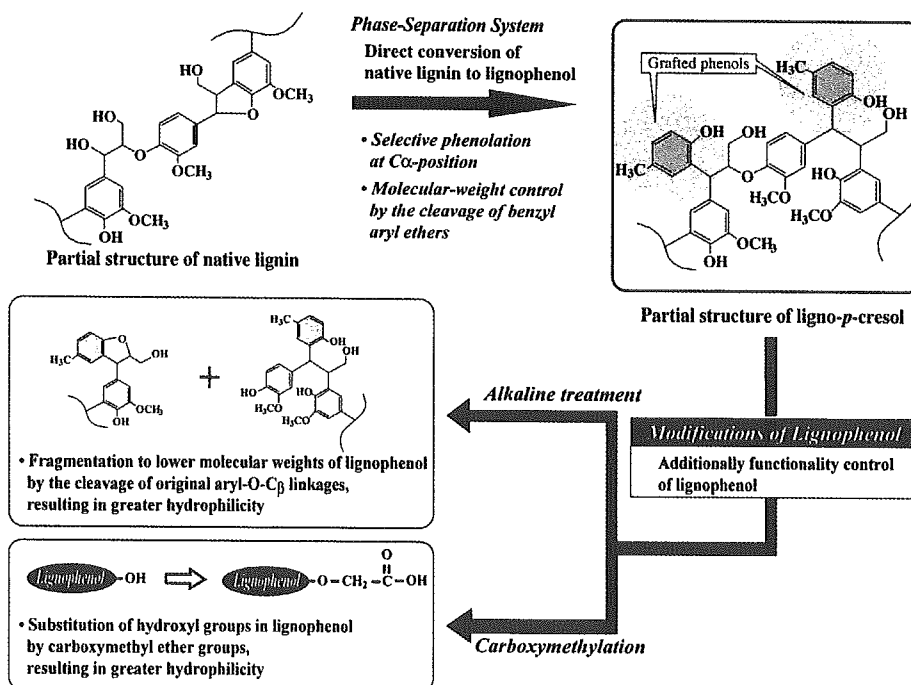


Figure 1. Conversion of native lignin into lignophenol derivatives and control of their functionality.

Table 1. Properties of lignophenol derivatives and the effect of various lignophenol derivatives on H₂O₂-induced apoptosis in SH-SY5Y cells

No.	Lignophenol derivatives	Properties of lignophenol derivatives			Antiapoptotic effect	
		Hydroxyl groups** (mol/C ₉)		Combined carboxymethyl groups*** (mol/C ₉)		Weight average molecular weight**** (\bar{M}_w)
		Phenolic OH	Total OH			
1	Lignin alkali	—	—	—	28,000	+
2	Lignopyrogallol (Japanese cedar)	3.61	4.27	—	3410	—
3	Lignocatechol (Japanese cedar)	2.78	3.46	—	4820	—
4	Lignoresorcinol (Japanese cedar)	2.66	3.37	—	4810	+
5	Lignopyrogallol (rice husk)	Not measured		—	1950	—
6	AT-lignopyrogallol (Japanese cedar)	3.11	3.63	—	2430	—
7	CM-lignocresol (rice husk)	0.62	1.53	0.60	3810	+
8	CM-lignocresol (bamboo)	0.46	1.31	0.66	5330	+++
9	CM-lignocresol (beech)	0.64	1.75	0.67	5460	+
10	CM- and AT-lignocresol* (beech)	0.63	1.77	0.75	1500	+
11	AT-lignocresol (beech)	1.21	2.18	—	1700	++

(-) No effect, (+) blockage 0–25%, (++) 25–50%, (+++) 50–100%.

AT—alkaline-treated, CM—carboxymethylated.

All lignophenol derivatives are water-soluble. (*) Carboxymethylated materials of the water-insoluble fraction of alkaline-treated lignocresol. (**) Hydroxyl groups of lignopolyphenols and CM-derivatives were determined by ¹H NMR spectra for original lignopolyphenols in CDCl₃-C₅D₅N (1:3, v/v) and their acetylated derivatives in CDCl₃ (containing TMS as the internal reference) and nonaqueous potentiometric titration, respectively. (***) Carboxy methyl groups were determined by nonaqueous potentiometric titration. (****) Average molecular weights were calculated by gel permeation chromatograms (columns; Shodex KF602, KF603, and KF604, eluent; tetrahydrofuran, detector; UV at 280nm) for acetylated derivatives, and which of lignin alkali was provided by technical data of Aldrich chemical company, Inc.

However, when water-insoluble lignophenols were carboxymethylated (CM) and/or alkaline-treated (AT), they became highly hydrophilic and water-soluble. Especially, CM-lignophenols showed a high binding affinity for proteins because of the introduced carboxyl groups.⁵ The carboxymethyl groups were recognized by ¹H NMR (Table 1) and IR spectroscopy (Fig. 2). Signals at δ 4.6 in the NMR spectra of CM-lignophenols (lig-8), which were absent in the original lignophenols, were due to the methylene protons of the –OCH₂COOH groups. As shown in Figure 2, absorption bands around 1600–1710 and 1425 cm⁻¹ in the IR spectra of CM-lignocresols were markedly increased in intensity compared with those of original lignophenols after phase-separation, due to the overlapped absorptions of introduced carboxyl groups and aromatic nuclei in the original ligno-

phenols (Fig. 2). The molecular weights of lignopolyphenols with or without AT and/or CM-lignophenols were within range of 1500–5500 or 2000–5000, respectively (Table 1).

2.2. Protective effects of lignophenol derivatives against the apoptosis induced by oxidative stress

We examined the ability of various lignophenol derivatives to protect SH-SY5Y cells from hydrogen peroxide (H₂O₂)-induced cell death. First, we determined the concentration of H₂O₂ required to induce apoptotic cell death by incubation for 12h and the concentrations of 75–100 μ M were found to be enough to induce apoptosis. The cell death induced by H₂O₂ at 100 μ M for 12h was found to be due to apoptosis, because the morphological findings characteristic of apoptosis such as nuclear condensation and fragmentation assessed by Hoechst 33342 nuclear staining, as well as DNA ladder formation were observed (Fig. 3). Next, we evaluated the apoptosis-blocking effect of various lignophenol derivatives (10–50 μ M) for 12h. To circumvent a direct effect of the compounds on externally added ROS in the medium, the compounds were added after the treatment with H₂O₂ for 2h. As shown in Table 1, 7 of the 11 lignophenol derivatives tested exhibited the protective activity in the H₂O₂-induced apoptosis at 30 μ M. The lignocresol derivatives were more potent in the neuroprotective activity compared with other lignophenols. Especially, the CM-lignocresol from bamboo named lig-8, displayed the most potent apoptosis-preventing activity at 20 and 30 μ M. We used this compound for the following experiments for comparison with epigallocatechin gallate (EGCG) from green tea, which has been reported to protect against neuronal cell death induced by oxidative stress.^{12,13,18} Lig-8 had no effect on the growth of SH-SY5Y cells at the concentrations of 10–50 μ M, whereas EGCG showed cytotoxicity at more

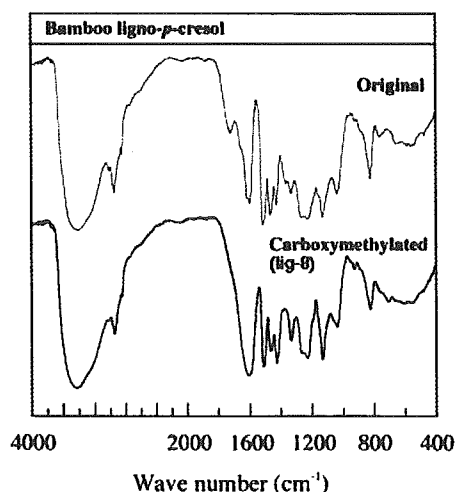


Figure 2. IR spectra of original (preparation after phase-separation) and carboxymethylated bamboo lignocresol derivative, lig-8.

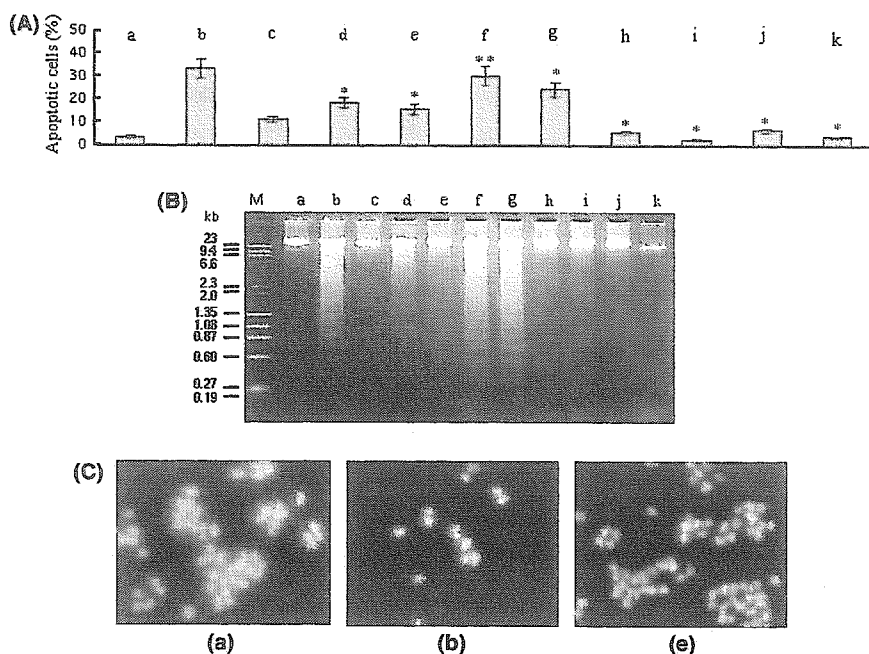


Figure 3. H₂O₂ or SIN-1-induced apoptosis and its blockage by the treatment with lig-8 or EGCG for 12 h in SH-SY5Y cells. (A) Apoptotic cell death evaluated by Hoechst 33342 staining. Results are the mean \pm SD of three independent experiments, * p <0.01; ** p <0.05 versus b or c. (B) Apoptotic cell death evaluated by DNA ladder formation. (a) Control (untreated cells); (b) H₂O₂ 100 μ M; (c) SIN-1 500 μ M; (d) H₂O₂ 100 μ M plus lig-8 20 μ M; (e) H₂O₂ 100 μ M plus lig-8 30 μ M; (f) H₂O₂ 100 μ M plus EGCG 10 μ M; (g) H₂O₂ 100 μ M plus EGCG 20 μ M; (h) SIN-1 500 μ M plus lig-8 20 μ M; (i) SIN-1 500 μ M plus lig-8 30 μ M; (j) SIN-1 500 μ M plus EGCG 10 μ M; (k) SIN-1 500 μ M plus EGCG 20 μ M. (C) Microscopic observation of cells treated with H₂O₂ alone (b) or H₂O₂ plus lig-8 (e) in Hoechst 33342 nuclear staining. Untreated control cells (a).

than 30 μ M (data not shown). Lig-8 significantly prevented H₂O₂-induced apoptosis at 20 or 30 μ M, whereas EGCG at 10 or 20 μ M exhibited a marginal antiapoptotic effect (Fig. 3A and B). In the case of apoptosis induced by 3-(4-morpholinyl)sydonimine (SIN-1)²⁰ which generates RNS in cells,²¹ lig-8 also exerted a potent protection against apoptosis at the same concentrations as in the H₂O₂-induced apoptosis. EGCG was more protective against SIN-1-induced apoptosis than H₂O₂-induced one (Fig. 3A and B).

In order to determine the site(s) of lig-8's action in the signaling pathway of apoptosis, we examined the activation of an apoptosis executioner caspase, caspase-3, by Western blot analysis. The 18-kD active form of caspase-3 was discernible at 6 h after the treatment with 100 μ M H₂O₂ (Fig. 4A). However, such active form was not detected in the paired sample from the cells treated with 100 μ M H₂O₂ in the presence of lig-8, suggesting that lig-8 blocked the caspase-3 activation. In order to further confirm the involvement of caspase-3 activation in apoptosis, we examined the effects of a caspase-3 inhibitor Z-DEVD-FMK and a pan-caspase inhibitor Z-VAD-FMK on apoptosis. It was shown that the inhibitors efficiently prevented the apoptosis in a concentration-dependent manner, as judged by Hoechst 33342 nuclear staining (Fig. 4B). The inhibitor almost blocked the apoptosis at 100 μ M. In addition, the activation of apoptosis initiator caspase-8 was clearly demonstrated by colorimetric protease assay (Fig. 5A) and dose-dependent apoptosis inhibition was shown by assay using a caspase-8 inhibitor Z-IETD-FMK (Fig. 5B). Thus, H₂O₂-induced apoptosis in SH-SY5Y cells

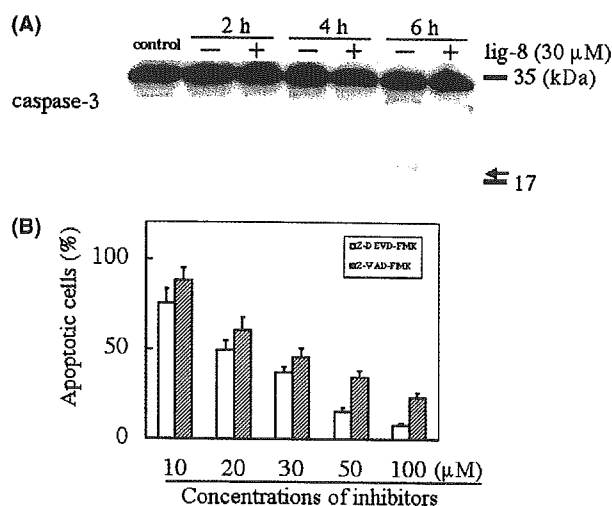


Figure 4. Involvement of caspase-3 activation in the H₂O₂-induced apoptosis and inhibition of caspase-3 activation by lig-8. (A) Western blot analysis of caspase-3. The arrow indicates the active form of caspase-3. (B) Apoptosis inhibition assay using caspase-3 inhibitor Z-DEVD-FMK or pan-caspase inhibitor Z-VAD-FMK. The apoptotic cell death was evaluated by Hoechst 33342 staining. Results are the mean \pm SD of three independent experiments. The percentage of apoptotic cells without the inhibitor is as 100%.

was exerted through the activation of both caspase-8 and -3. However, lig-8 did not affect the activation of caspase-8 (Fig. 5A).

In the apoptosis inhibition assay using pan-caspase or caspase-3 inhibitor, addition of lig-8 reduced the dose

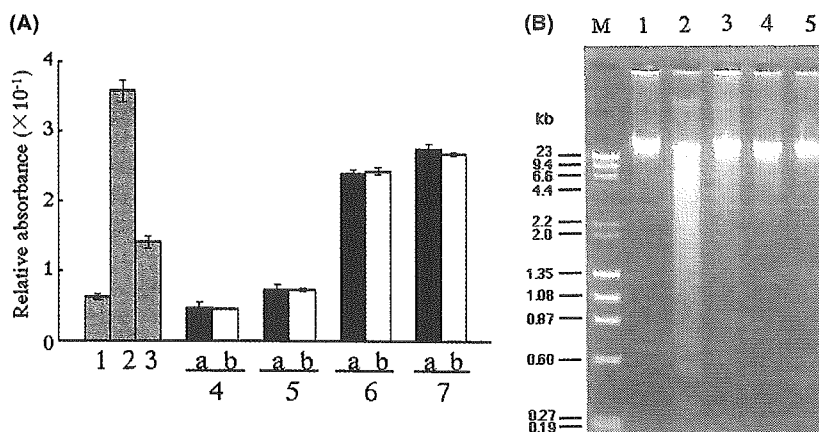


Figure 5. Involvement of caspase-8 in the H_2O_2 -induced apoptosis examined by colorimetric protease assay and apoptosis inhibition assay using Z-IETD-FMK in SH-SY5Y cells. (A) Colorimetric protease assay of caspase-8 in H_2O_2 -induced apoptosis. Each sample was prepared described in Experimental. Column 1, Jurkat cells without treatment; 2, Jurkat cells treated with ant-Fas antibody for 3h; 3, Jurkat cells treated with ant-Fas antibody in the presence of caspase-8 inhibitor (Z-IETD-FMK); (columns 4–7: (a) treatment with 100 μ M H_2O_2 , (b) treatment with 100 μ M H_2O_2 plus 30 μ M lig-8); 4, SH-SY5Y cells before treatment; 5, treated for 2h; 6, treated for 4h; 7, treated for 6h. The values of absorbance at 405nm are expressed. Means \pm SD of three independent experiments are given. (B) Activation of caspase-8 in SH-SY5Y cells examined by apoptosis inhibition assay. Three micrograms of DNA was applied onto each lane. The inhibitor for caspase-8, Z-IETD-FMK, was added 6h before exposure to 100 μ M H_2O_2 . The rescue of cell death was evaluated at 12h after 100 μ M H_2O_2 exposure by reduced formation of nucleosomal DNA fragments at each concentration of the inhibitor. Lane 1, DNA from cells in the presence of 0.01% DMSO and 60 μ M Z-IETD-FMK (control); lane 2, treatment with 100 μ M H_2O_2 for 12h; lane 3, with 100 μ M H_2O_2 plus 20 μ M inhibitor; lane 4, with 40 μ M inhibitor; lane 5, with 60 μ M inhibitor. Lane M is a DNA size marker.

of Z-DEVD-FMK or Z-VAD-FMK to exert the equivalent antiapoptotic efficacy (data not shown). These results led us to explore the *in vitro* effect of lig-8 in the process of procaspase-3 proteolysis. Lig-8 was added to the reaction mixture containing SH-SY5Y cell lysate and the recombinant active caspase-8 in tubes, and its effect on caspase-3 activation was examined by Western blot analysis. Lig-8 dose-dependently prevented the proteolysis of procaspase-3 by recombinant active caspase-8 (Fig. 6A). Indeed, the higher concentrations of lig-8 were needed to suppress the activation of caspase-8, but the results from *in vivo* and *in vitro* experiments suggested that lig-8 possibly blocked the activation of caspase-3.

In the last several years, it has become increasingly clear that mitochondria play a major rate-limiting role in the apoptosis of neuronal cells. The decision/effector phase of the apoptotic process converges on mitochondria, where permeabilization of mitochondrial membranes occurs as a result of the permeability transition pore complex (PTPC).^{22,23} We next examined the effect of lig-8 on mitochondrial membrane PT in the apoptosis. The mitochondrial membrane potential examined by FACS clearly showed a decrease in the cells treated with H_2O_2 for 8h and its decrease was significantly reduced in the presence of lig-8 (Fig. 7A). Furthermore, the release of cytochrome c from mitochondria and simultaneously the sequential activation of caspase-9 were also

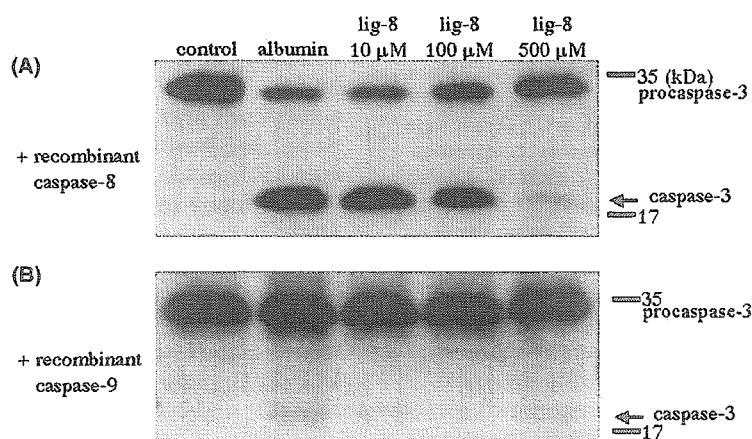


Figure 6. Effect of lig-8 on proteolytic cleavage of procaspase-3 by recombinant caspase-8 or caspase-9 *in vitro* examined by Western blot analysis. (A) Proteolysis of procaspase-3 by recombinant caspase-8. (B) The proteolysis of procaspase-3 by recombinant caspase-9. The cell lysate without recombinant caspase-8 is used as a negative control. We added albumin to reaction buffer as a positive control.

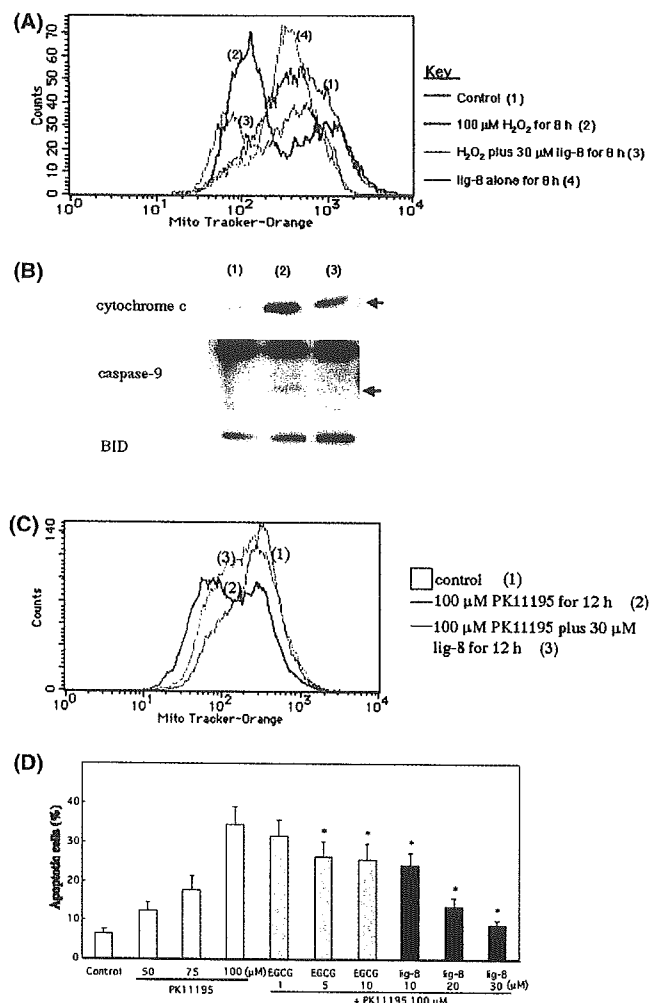


Figure 7. Effect of lig-8 on mitochondrial membrane potential and release of cytochrome c in the H_2O_2 - or PK11195-induced apoptosis. (A) Mitochondrial membrane potential examined by FACS using Mito-Tracker Orange or Green. The cells were treated for 8 h with 100 μM H_2O_2 (trace 2), 100 μM H_2O_2 plus 30 μM lig-8 (trace 3), or lig-8 alone (trace 4). Control (trace 1) is untreated cells. The patterns of fluorescence intensity of Mito-Tracker Green were almost similar in the samples tested. (B) Western blot analysis of cytochrome c, caspase-9, and BID at 8 h after the treatment with 100 μM H_2O_2 (lane 2) or 100 μM H_2O_2 plus 30 μM lig-8 (lane 3). Lane 1 is untreated cells (control). The lane numbers correspond to the same numbers in (A). (C) Mitochondrial membrane potential in PK11195-induced apoptosis examined by FACS using Mito-Tracker Orange or Green. The cells were treated for 12 h with 100 μM PK11195 (trace 2) or 100 μM PK11195 plus 30 μM lig-8 (trace 3). Control (trace 1) is untreated cells. The patterns of fluorescence intensity of Mito-Tracker Green were almost similar in the samples tested. (D) Comparison of the apoptosis-inhibitory activity between lig-8 and EGCG in PK11195-induced apoptosis evaluated by Hoechst 33342 nuclear staining. Results are the mean \pm SD of three independent experiments, * $p < 0.01$ versus the value of apoptotic cells (%) in 100 μM PK11195 treatment.

suppressed by lig-8 (Fig. 7B). Thus, H_2O_2 -induced apoptosis is considered to be mediated via the mitochondrial pathway, and lig-8 was shown to ameliorate the apoptosis by preventing depolarization of mitochondrial membrane PT. The truncated BID, which induces the release of cytochrome c from mitochondria without mitochondria potential loss,²³ was not observed by Western blot analysis (Fig. 7B). Considering the time course of the

apoptosis, the activation of caspase-8/3 likely affects the mitochondrial pathway.

In order to further assess the effect of lig-8 on mitochondrial membrane PT, we examined the changes in mitochondrial membrane potential induced by a peripheral benzodiazepine receptor (PBR) ligand, 1-(2-chlorophenyl)-N-(1-methylpropyl)-3-isoquinolinecarboxamide (PK11195).^{24,25} FACS demonstrated that the decrease in mitochondrial membrane potential by 100 μM PK11195 was considerably prevented by lig-8 at 30 μM (Fig. 7C). Moreover, the activation of caspase-9 by PK11195 was almost blocked by 30 μM lig-8 (data not shown) and therefore, lig-8 significantly inhibited the apoptosis in a concentration-dependent manner, whereas EGCG only slightly inhibited the PK11195-induced apoptosis (Fig. 7D). Thus, lig-8 was able to prevent PK11195-induced cell death mediated by mitochondrial membrane PT, as observed in H_2O_2 -induced cell death. Based on these data, we also examined the effect of lig-8 on in vitro proteolysis of the recombinant active caspase-9, and showed that lig-8 prevented proteolysis of pro-caspase-3 (Fig. 6B). Taken together, these data suggest that the antiapoptotic effect of lig-8 was most likely due to its action on the caspase-3 proteolytic process by caspase-8 and -9, and also on depolarization of mitochondrial membrane PT.

The level of intracellular ROS measured by FACS using CM- H_2 DCF-DA at 2 h after the treatment with H_2O_2 was slightly increased. However, the level in H_2O_2 /lig-8- and H_2O_2 /EGCG-cotreated cells was reduced, indicating that lig-8 as well as EGCG exerted an ROS-scavenging effect (Fig. 8A, right panel). Even though the level of intracellular ROS at 30 min after the treatment compensatively decreased in the H_2O_2 -treated cells (Fig. 8A, left panel), the ROS scavenging activity of lig-8 was also observed. Perhaps the ROS scavenging activity of lig-8 is more potent than that of EGCG. These results were consistent with those in in vitro ROS-scavenging test (Fig. 8B, left panel). EGCG may scavenge more NO radicals compared with lig-8 in in vitro ROS-scavenging test (Fig. 8B, right panel), which possibly reflected the results of cell death assay in Figure 3A.

The results in the present study have provided the first demonstration that lignophenol derivatives protected human dopaminergic neuroblastoma SH-SY5Y cells against cell death due to apoptosis induced by oxidative stress. We were successful in converting the native lignins to bioactive lignophenols, which have almost original 3-dimensional network structures by using the phase-separation technique. Among various lignophenols, lignocresol derivatives exhibited higher apoptosis-blocking activity than other lignophenols tested. Lig-8, the water-soluble carboxymethylated (CM)-lignocresol from bamboo, displayed the most potent preventive effect on the apoptosis induced by oxidative stress such as H_2O_2 and NO in SH-SY5Y cells.

Native lignin has various complex structures with inter-unit linkages, polyphenolic groups, and a 3-dimensional branched network. Furthermore, the chemical proper-

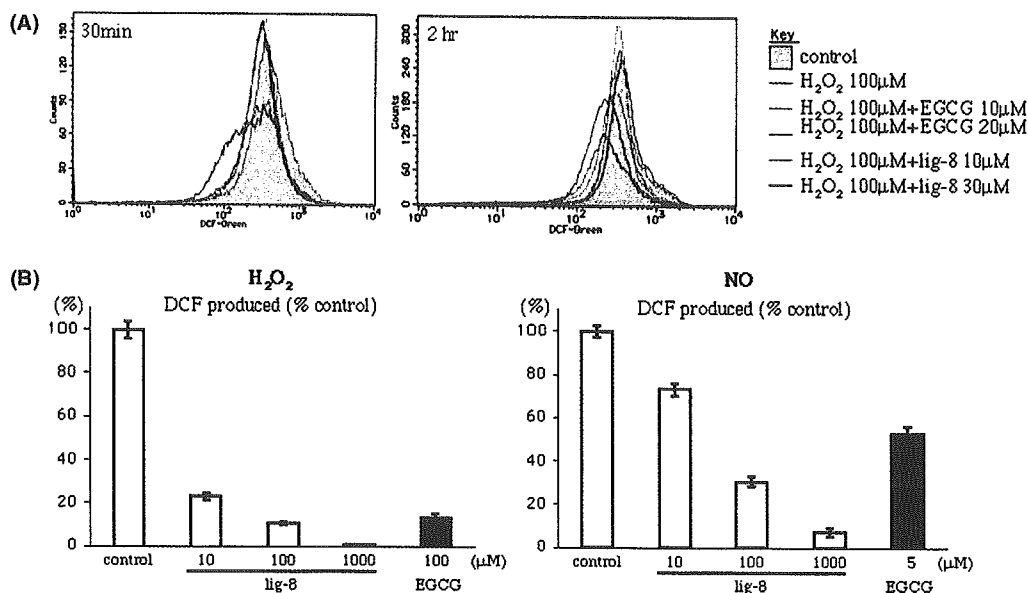


Figure 8. Antioxidant activity of lig-8. (A) The intracellular ROS levels scavenged by EGCG or lig-8 after H₂O₂-treatment in SH-SY5Y cells was measured by FACS as described in Experimental. The cells in the medium without FCS were treated with 100 μM H₂O₂ for 30 min or 2 h. (B) The levels of ROS generated from H₂O₂ or a nitric oxide donor, Nor-4, were quantified by measuring the fluorescence intensity of DCF, and the scavenging potencies of EGCG and lig-8 were expressed as the percentage of control without the antioxidants. The average of two independent measurements is given.

ties of lignins, especially the network structures, differ greatly depending on the lignocellulosics, because the precursors bulging up lignin differ in their species. Generally, softwood lignins consist mainly of guaiacyl aromatic units, and hardwood lignins contain evenly guaiacyl and syringyl units. On the other hand, herb lignins including bamboo have parahydroxy phenyl units rather than these units. Certainly, the structure containing the parahydroxy phenyl units in bamboo lignin and the additional phenolic groups may contribute to the neuroprotective activity of lig-8. However, further studies of the structure–activity association are necessary to determine the units or groups involved in the activity.

The apoptosis induced by H₂O₂ in SH-SY5Y cells was mediated by activation of caspase-3, which was confirmed by Western blot analysis and the apoptosis inhibition assay using the caspase-3 inhibitor Z-DEVD-FMK or pan-caspase inhibitor Z-VAD-FMK. Lig-8 significantly prevented activation of caspase-3 at 6 h after the treatment with H₂O₂. The apoptosis was completely blocked by the incubation with either 100 μM Z-VAD-FMK or Z-DEVD-FMK. Addition of various concentrations of lig-8 to the inhibitor clearly reduced amount of the inhibitors in dose-dependent manner to compensate the apoptosis-blocking ability in 100 μM of the inhibitor (data not shown). These results raise the possibility that lig-8 may directly block the activation of caspase-3 and/or other caspases. Then, we examined the activation of caspase-8, as an initiator caspase of apoptosis, which acts upstream of procaspase-3. By colorimetric protease assay using substrate of caspase-8, we found that the activation of caspase-8 is involved in the apoptosis. However, we could not obtain the positive data that lig-8 affects the activation. In the light of these data, we examined the proteolysis blocking effect

of lig-8 on caspase-3 activation in vitro and found that lig-8 blocked the proteolysis of procaspase-3 by recombinant active caspase-8 in a dose-dependent manner. However, the higher concentrations of lig-8 were needed to see inhibition in caspase-3 activation, compared with those of in vivo. Therefore, although it can be considered that lig-8 rescues cells from the apoptosis by inhibiting the activation of caspase-3 via caspase-8, antiapoptotic effect of lig-8 is at least in part mediated through caspase-8/3. Similarly, the in vitro proteolysis inhibition assay using the recombinant active caspase-9 showed the ability of lig-8 to inhibit the proteolytic cleavage of procaspase-3. To define the specificity of lig-8's action to inhibit procaspase-3 proteolysis via caspase-8 or -9, further experiments are required.

It has been earlier reported that the caspase-8 activation is mediated by induction of Fas expression in H₂O₂-induced apoptosis in B-cell lymphoma cells.²⁶ However, we did not obtain any evidence causing caspase-8 activation in the H₂O₂-induced apoptosis.

On the other hand, lig-8 significantly prevented the depolarization of mitochondrial membrane potential at 8 h after the treatment, as judged by FACS analysis using Mito-Tracker fluorescent probes. Moreover, Western blot analysis of cytochrome c indicated marked suppression of cytochrome c release from mitochondria by lig-8. In order to further confirm lig-8's action on mitochondrial membrane PT, we examined the effect of lig-8 in PK1195-induced apoptosis involving the loss of mitochondrial membrane PT.^{24,25} As observed in H₂O₂-induced apoptosis, lig-8 considerably protected the cells from PK1195-induced apoptosis by preventing the loss of PT. Lig-8 may affect the interaction of PK1195 with peripheral benzodiazepine receptor

(PBR), in part, by competitive inhibition. In Bcl-2-over-expressing SH-SY5Y cells, PK11195-induced apoptosis was completely blocked (data not shown). Therefore, its mode of prevention of apoptosis was different from that by lig-8, suggesting that the PBR receptor on the mitochondrial membrane may be closely associated with molecules of PTPC including Bcl-2/Bax and VDAC.²⁷ Thus, lig-8 prevents the depolarization of mitochondrial membrane PT in both cases. Since the caspases-8/3 pathway (6 h after H₂O₂-treatment) precedes the mitochondrial pathway (8 h after H₂O₂-treatment), it is suggested that the activation of caspase-8/3 may affect the mitochondrial pathway via caspase-2.^{28,29} In fact, the caspase-2 inhibitor Z-VAD-FMK significantly blocked the apoptosis dose-dependently, however, lig-8 did not affect the activation of caspase-2 (data not shown) and the truncated BID acting on mitochondria was not observed.

As for the antioxidant activity of lig-8, we have demonstrated that the intracellular ROS level of H₂O₂-treated cells was decreased by addition of lig-8. Its scavenging activity was also shown in in vitro ROS-scavenging test and even on superoxide (data not shown). Therefore, lig-8 likely exerts its protective activity by scavenging ROS. In comparison with EGCG, which has been reported to exert neuroprotective effect because of its antioxidant activity,^{12,13,18} lig-8 attenuated the cell death induced by either H₂O₂ or nitric oxide free radical donor SIN-1 in SH-SY5Y cells. In addition, our data suggest that EGCG may scavenge RNS produced by NO generating agent SIN-1-rather than ROS by H₂O₂-treatment. Since the preventive effect of lig-8 is mainly due to blockage of the apoptotic signaling pathway, the mechanism(s) underlying preventive effect for cell death by lig-8 seems likely to be different from that by EGCG.

Recently, some phytochemicals are considered to be beneficial for prevention of neuronal cell death by affecting the intracellular signal transduction pathway. EGCG has protective effects against A β -induced apoptosis through regulation of the secretory process of non-amyloidogenic amyloid precursor protein via protein kinase C (PKC).³⁰ Quercetin prevents the H₂O₂-mediated mitochondrial dysfunction by preserving mitochondrial membrane PT as well as an increased in expression of BCL-2 and BCL-X(L) in cardiomyoblast cells.³¹ It was also reported that quercetin exhibits a protective action against NO-induced toxicity via PKC pathway in cultured rat hippocampal cells.³² In our cases, the levels of phosphorylated ERK and p38 were changed, but they were not affected by lig-8.

Lig-8 also exhibited an antiapoptotic activity against H₂O₂-induced apoptosis even in rat neuroblastoma cell line PC12. More extensive studies are necessary for elucidation of the apoptosis-inhibitory activity of lig-8 in primary cultured neuronal cells and in animal models, which are under current progress in our laboratory. Lig-8 is considered to exhibit a more potent neuroprotective effect compared with EGCG because of the direct action on apoptosis signal pathways. The results of our current study suggest that lignocresol derivatives would

be a candidate for agent to rescue the neuronal cells from cell death induced by the oxidative stress that accelerates the progression of neurodegenerative diseases.

3. Conclusion

In the present work it was demonstrated that by using our newly developed phase-separation technique lignin, a durable aromatic network polymer second to cellulose in abundance was able to be converted into highly active lignophenol derivatives with antioxidant activity. These lignophenol derivatives were found to show the potent neuroprotective activity against oxidative stress. Among the compounds examined, a lignocresol derivative from bamboo (lig-8) exhibited the most potent neuroprotective activity against hydrogen peroxide (H₂O₂)-induced apoptosis in human neuroblastoma cell line SH-SY5Y by preventing the caspase-3 activation via either caspase-8 or caspase-9. Furthermore, it was found that lig-8 exerted the antiapoptotic effect by inhibiting dissipation of the mitochondrial membrane permeability transition induced by H₂O₂ or by the peripheral benzodiazepin receptor ligand PK11195. These data suggest that lig-8 is a promising neuroprotector, which affects the signaling pathway of neuronal cell death and that it would be of benefit to delay the progress of neurodegenerative diseases.

4. Experimental

4.1. Lignocellulosics and lignin preparation

Air-dried lignocellulosics (softwood, Japanese cedar [*Cryptomeria japonica*]; hardwood, Japanese beech [*Fagus crenata*]; herbs, rice husk [*Oryza sativa*], and bamboo [*Phyllostachys bambusoides*]) were milled until they could pass through a 100 μ m screen and then extracted with ethanol–benzene (1:2, v/v) for 48 h. Extracts of these lignocellulosics were air-dried to remove the solvent and then the extract were treated with pepsin solution by Ellis's method³³ to prepare their protein-free form. Lignin alkali (Aldrich Chemical Co. Inc., WI) was used as conventional lignin, kraft lignin.

4.2. Synthesis and isolation of lignophenol

Using a modified phase-separation system (Two-step process I) (Fig. 1),² we synthesized water-insoluble ligno-*p*-cresol and water-soluble ligno-catechol, -resorcinol, and -pyrogallol. These phenols (monohydric phenol *p*-cresol and polyhydric phenols catechol, resorcinol, and pyrogallol; 3 mol/C9 [C9 is lignin building unit]) were sorbed to extract solvent-free wood or protein-free herb meals. Sulfuric acid (72%, 20 mL/g lignocellulosics) was added to the lignocellulosics-sorbed phenols, and the mixture was vigorously stirred at room temperature for 1 h. Phenol–benzene solution (7:3, v/v) was added to the mixture with stirring. After stirring, the reaction mixture was separated into two phases, organic and aqueous phases. The organic phase was taken up and then an excess amount of ethyl ether was added drop-

wise with vigorous stirring. The resultant precipitates were dissolved in acetone and the insoluble substance was removed. The aqueous phase was mixed with excess water and centrifuged. The supernatant was neutralized with NaOH, dialyzed, and freeze-dried. The dried material was extracted with methanol, and then the soluble fraction was added dropwise to an excess amount of ethyl ether with stirring. The precipitate (water-soluble lignophenol) was collected by centrifugation and dried over P₂O₅ after evaporating the solvent.

4.3. Selective cleavage of lignophenols by alkaline treatment

The aryl ether linkages of lignophenols were selectively cleaved by alkaline treatment.² For this, water-insoluble ligno-*p*-cresol from the organic phase was treated with 0.5 N NaOH (20 mL/g lignophenol) at 170 °C for 1 h and the reaction mixture was then acidified to pH 2 with 1 N HCl and centrifuged. The resultant precipitate (water-insoluble fraction) was collected by centrifugation, washed several times, and dried over P₂O₅. The supernatant (water-soluble fraction) was dialyzed and freeze-dried.

4.4. Carboxymethylation of lignophenol

Water-insoluble lignocresol from the organic phase or water-insoluble fraction of alkaline-treated lignocresol was dissolved in isopropanol (IPA, 4 g/g lignophenol), and 40 % NaOH (2.5 g/g lignophenol) was added with stirring. Then, monochloroacetic acid (1.6 mol/mol hydroxyl group in lignophenol) in isopropanol (4 g/g lignophenol) was added and stirred further at 50 °C for 2 h. The resultant precipitate including carboxymethylated (CM-) lignophenols was collected by centrifugation, dissolved in water, and acidified to pH 2. The insoluble fraction was removed by centrifugation and the supernatant containing the water-soluble CM-lignophenols was dialyzed and then freeze dried.

4.5. Structural analysis of lignophenols

The amounts of combined phenols and hydroxyl groups in the lignophenols were calculated from ¹H NMR spectra of acetylated lignophenols obtained with a JEOL JNM-LA300 FT-NMR. *p*-Nitrobenzaldehyde was used as the internal reference for their determination. The extents of the carboxymethylation were estimated by infrared (IR) spectroscopy (KBr disks, JASCO FT/IR-8900 m) and NMR spectroscopy. The average molecular weights were measured by gel permeation chromatography on a JASCO GULLIVER 1500 system, PU-1585, UV-1570 with two columns (Shodex OH-pak SB-803 HQ, SB-806M HQ). Sodium chloride (10 μM) was used as the eluent.

4.6. Cell culture and treatment of SH-SY5Y

Human neuroblastoma cell line SH-SY5Y was cultured in MEM supplemented with 5% fetal calf serum (FCS) and maintained at a density of 2 × 10⁵ cells per mL before treatment. For the experiments, the cells were seeded at

the density of 1–2 × 10⁵/mL in 60 mm diameter wells and cultured for 12 h. After the cells were pretreated with hydrogen peroxide (H₂O₂; Wako, Tokyo), 3-(4-morpholinyl)sydonimine (SIN-1; Dojindo, Kumamoto, Japan), and 1-(2-chlorophenyl)-N-(1-methylpropyl)-3-isoquinolinecarboxamide (PK11195; TOCRIS, MO) for 2 h, agents such as lignophenol derivatives and epigallocatechin gallate (EGCG; Wako) were added to the cell cultures at selected concentrations.

4.7. Assessment of apoptosis

For assessment of the morphological characteristics of apoptosis, the cells were stained with Hoechst 33342 (5 μg/mL) at 37 °C for 30 min, washed once with PBS, resuspended and pipetted dropwise onto a glass slide, and examined by fluorescence microscopy using an Olympus microscope (Tokyo, Japan) equipped with an epi-illuminator and appropriate filters. The cells with condensed and fragmented nuclei stained with Hoechst 33342 were assessed to be apoptotic. In all conditions examined, necrotic cell death by H₂O₂ was negligible (less than 2% of the total cells). Approximately 200 cells were counted in four different fields and three independent experiments were performed. To examine nucleosomal DNA fragmentation by agarose gel electrophoresis, cellular DNA was extracted from whole cells by ethanol precipitation after phenol/chloroform preparation. RNase was added to the DNA solution at the final concentration of 20 μg/mL, and the mixture was incubated at 37 °C for 30 min. After electrophoresis on a 2.5% agarose gel, DNA was visualized by ethidium bromide staining. For the apoptosis inhibition assay, a caspase-3 inhibitor, Z-DEVD-FMK (MBL, Nagoya, Japan), a pan-caspase inhibitor, Z-VAD-FMK (MBL), a caspase-8 inhibitor, Z-IETD-FMK (MBL), or a caspase-2 inhibitor, Z-VDVAD-FMK (Sigma, Saint Louis, MO) was added at the desired concentrations to the medium 30 min before the H₂O₂ treatment.

4.8. Western blot analysis

SH-SY5Y cells were washed twice with PBS, suspended in lysis buffer A or B and then homogenized. Lysis buffer A (2 × PBS, 0.1% SDS, 1% Nonidet P-40, 0.5% sodium deoxycholate, and 25 × complete, protease inhibitor (Roche, Penzberg Germany)) was used to analyze caspases and BID. Lysis buffer B (250 mM sucrose, 20 mM Hepes-KOH (pH 7.5), 10 mM KCl, 1.5 mM MgCl₂, 1 mM EDTA, 1 mM EGTA, 1 mM DTT, and 25 × Complete) was used to analyze AIF and cytochrome c. The mitochondrial and cytosolic fractions were prepared by the centrifugation after the incubation with Lysis buffer B. Five micrograms of lysate protein was separated by SDS-PAGE using a 12% polyacrylamide gel and electroblotted onto a PVDF membrane (Du Pont, Boston, MA). After blockage of nonspecific binding sites for 1 h with 5% nonfat milk in PBS containing 0.1% Tween 20, the membrane was incubated overnight at 4 °C with antihuman caspase-3 (Transduction Laboratories, Lexington, KY), antihuman caspase-9 (MBL), antihuman cytochrome c (R&D Systems, Minneapolis,

MN), or antihuman BID (R&D Systems) antibody. The membranes were then washed three times with PBS containing 0.1% Tween 20, incubated further with alkaline phosphatase-conjugated goat antimouse antibody (Promega, Madison, WI) at room temperature, and then washed three times with PBS containing 0.1% Tween 20. The immunoblots were visualized by use of an enhanced chemiluminescence detection kit (New England Biolabs, Beverly, MA).

4.9. In vitro proteolysis of procaspase-3 by caspase-8 or -9

Protein (1 μ g) of SH-SY5Y cell lysate was incubated at 37°C for 1 h with 1 unit or 3 units of recombinant caspase-8 (MBL) or -9 (MBL), respectively, in the solution containing 50 mM Hepes (pH 7.2), 50 mM NaCl, 0.1% Chaps, 10 mM EDTA, 5% glycerol, and 10 mM DTT. The proteolytic cleavage was assessed by Western blot analysis.

4.10. Measurement of mitochondrial membrane potential

Mitochondrial membrane potential was measured by use of the fluorescent dyes, Mito-Tracker Green (Molecular Probes, #M-7514, Eugene, OR) estimating the mitochondrial volume, and Mito-Tracker Orange (Molecular Probes, #M-7511), which accumulates selectively in active mitochondria. After the cells were washed twice with RPMI-1640 medium, the treated or untreated cells were incubated with Mito-Tracker fluorescent probes (100 nM each) for 30 min at 37°C. Then the cells were collected, washed twice with PBS, and resuspended in PBS. The fluorescence of Mito-Tracker Orange and Green was analyzed by fluorescence activated cell sorter (FACS; Becton Dickinson, San Jose, CA).

4.11. Measurements of production and scavenging activity of reactive oxygen or reactive nitrogen species

The production of reactive oxygen species (ROS) was monitored by the use of 5-(and-6)-chloromethyl-2',7'-dichlorodihydrofluorescein diacetate (CM-H₂ DCF-DA; Molecular Probes, Irvine, CA) or 2',7'-dichlorodihydrofluorescein diacetate (H₂ DCF-DA; Molecular Probes). After the cells treated with or without H₂O₂ were washed twice with PBS, CM-H₂ DCF-DA (10 μ M) was added to the cell suspension in PBS at 37°C. After 30 min-incubation, the 2',7'-dichlorodihydrofluorescein (DCF) in cells was determined by the FACS. The fluorometric measurement was performed with excitation and emission wavelengths of 495 and 530 nm, respectively. For the measurement of the in vitro ROS scavenging potency, ROS was produced in a 96-well microplate by incubation of 1 mM H₂O₂ or 1 mM nitric oxide donor, Nor-4 (Dojindo) in PBS at 37°C and the effects of lig-8 or EGCG were examined by addition of their various concentrations. The increase of a fluorescent product, DCF from H₂ DCF-DA was followed in a MTP-600F (CORONA electronic, Hitachinaka, Japan) reader with excitation at 495 and 530 nm emission.

4.12. Colorimetric protease assay

The activation of caspase-8 was determined by colorimetric protease assay. Briefly, the cells treated with H₂O₂ were harvested at the indicated times, suspended in cell lysis buffer, and then incubated on ice for 10 min. The lysate containing 150 μ g protein was incubated with 200 μ M IETD-pNA substrate (MBL) at 37°C for 2 h. Levels of released pNA were measured with a Nalgenunc spectrofluorometer at 405 nm. The cell lysate of Jurkat cells treated with anti-Fas antibody (clone CH-11) (MBL) for 3 h was used as a positive control for caspase-8 activation.

4.13. Statistical analysis

For the statistical analyses, 1-way ANOVA and Fisher's PLSD test were performed by using StatView software (SAS Institute Inc., Cary, NC).

Acknowledgements

We thank Ms. Nishizawa for her skillful assistance for these experiments. This work was supported by a grant from Medical Frontier Strategy Research (W.M., Y.A., and M.N.) from the Ministry of Health, Labor and Welfare, Japan.

References and notes

- Funaoka, M.; Abe, I. *Tappi J.* **1989**, *72*, 145.
- Funaoka, M.; Fukatsu, S. *Holzforchung* **1996**, *50*, 245.
- Funaoka, M.; Matsubara, M.; Seki, N.; Fukatsu, S. *Biotechnol. Bioeng.* **1995**, *46*, 545.
- Funaoka, M.; Ioka, H.; Hoshio, T.; Tanaka, Y. *J. Network Polym.* **1996**, *17*, 121.
- Suzuki, H.; Tochikura, T. S.; Iiyama, K.; Yamazaki, S.; Yamamoto, N.; Toda, S. *Agric. Biol. Chem.* **1989**, *53*, 3369–3372.
- Ichimura, T.; Watanabe, O.; Maruyama, S. *Biosci. Biotechnol. Biochem.* **1998**, *62*, 575.
- Jiang, Y.; Satoh, K.; Aratsu, C.; Kobayashi, N.; Unten, S.; Kakuta, H.; Kikuchi, H.; Nishikawa, H.; Ochiai, K.; Sakagami, H. *Anticancer Res.* **2001**, *21*, 965.
- Thompson, C. B. *Science* **1995**, *267*, 1456.
- Tatton, W. G.; Chalmes-Redman, R. M. E. *Ann. Neurol.* **1998**, *44*(Suppl 1), S134.
- Kidd, P. M. *Altern. Med. Rev.* **2000**, *5*, 502.
- Conrad, C. C.; Marshall, P. L.; Talent, J. M.; Malakowsky, C. A.; Choi, I.; Gracy, R. W. *Biochem. Biophys. Res. Commun.* **2000**, *275*, 678.
- Lee, S. R.; Im, K. J.; Suh, S. I.; Jung, J. G. *Phytother. Res.* **2003**, *17*, 206.
- Nagai, K.; Jiang, M. H.; Hada, J.; Nagata, T.; Yajima, Y.; Yamamoto, S.; Nishizaki, T. *Brain Res.* **2002**, *956*, 319.
- Dona, M.; Dell'Aica, I.; Calabrese, F.; Benelli, R.; Morini, M.; Albini, A.; Garbisa, S. *J. Immunol.* **2003**, *170*, 4335.
- Singh, R.; Ahmed, S.; Malemud, C. J.; Goldberg, V. M.; Haqqi, T. M. *J. Orthop. Res.* **2003**, *21*, 102.
- Jung, Y. D.; Kim, M. S.; Shin, B. A.; Chay, K. O.; Ahn, B. W.; Liu, W.; Bucana, C. D.; Gallick, G. E.; Ellis, L. M. *Br. J. Cancer* **2001**, *84*, 844.
- Sachinidis, A.; Seul, C.; Seewald, S.; Ahn, H.; Ko, Y.; Vetter, H. *FEBS Lett.* **2000**, *471*, 51.

18. Mira, L.; Fernandez, M. T.; Santos, M.; Rocha, R.; Florencio, M. H.; Jennings, K. R. *Free Radical Res.* **2002**, *36*, 1199.
19. Nanami, O.; Watanabe, Y.; Syuto, B.; Nakano, M.; Tsuji, M.; Kuwabara, M. *Free Radical Res.* **1998**, *29*, 359.
20. Oh-hashi, K.; Maruyama, W.; Yi, H.; Takahashi, T.; Naoi, M.; Isobe, K. *Biochem. Biophys. Res. Commun.* **1999**, *263*, 504.
21. Feelisch, M.; Ostrowski, J.; Noack, E. *J. Cardiovasc. Pharmacol.* **1989**, *14*, S13.
22. Zoratti, M.; Szabo, I. *Biochem. Biophys. Acta* **1995**, *1241*, 139.
23. Tsujimoto, Y.; Shimizu, S. *FEBS Lett.* **2000**, *466*, 6.
24. Vrabec, J. P.; Lieven, C. J.; Levin, L. A. *Invest. Opth. Vis. Sci.* **2003**, *44*, 2774.
25. Solary, E.; Bettaieb, A.; Dubrez-Daloz, L.; Corcos, L. *Leukemia. Lymphoma* **2003**, *44*, 563.
26. Devadas, S.; Hinshaw, J. A.; Zaritskaya, L.; Williams, M. S. *Free Radical Biol. Med.* **2003**, *35*, 648.
27. Shimizu, S.; Narita, M.; Tsujimoto, Y. *Nature* **1999**, *399*, 483.
28. Lopez, E.; Ferrer, I. *Brain Res. Mol. Brain Res.* **2000**, *85*, 61.
29. Guo, Y.; Srinivasula, S. M.; Druilhe, A.; Fernandes-Alnemri, T.; Alnemri, E. S. *J. Biol. Chem.* **2002**, *277*, 13430.
30. Levites, Y.; Amit, T.; Mandel, S.; Youdim, M. B. *FASEB J.* **2003**, *17*, 952.
31. Park, C.; So, H. S.; Shin, C. H.; Baek, S. H.; Moon, B. S.; Shin, S. H.; Lee, H. S.; Lee, D. W.; Park, R. *Biochem. Pharmacol.* **2003**, *66*, 1287.
32. Bastianetto, S.; Zheng, W. H.; Quirion, R. *Br. J. Pharmacol.* **2000**, *131*, 711.
33. Ellis, G. H. *J. Assoc. Agric. Chem.* **1949**, *32*, 287.

—Original—

Long-Term Treatment Effects of *Pueraria mirifica* Phytoestrogens on Parathyroid Hormone and Calcium Levels in Aged Menopausal Cynomolgus Monkeys

Hataitip TRISOMBOON^{1,2}, Suchinda MALAIVIJITNOND², Juri SUZUKI³, Yuzuru HAMADA³, Gen WATANABE^{4,5} and Kazuyoshi TAYA^{4,5}

¹Biological Science Ph.D. Program, Faculty of Science, Chulalongkorn University, Bangkok 10330, ²Primate Research Unit, Department of Biology, Faculty of Science, Chulalongkorn University, Bangkok 10330, Thailand, ³Primate Research Institute, Kyoto University, Inuyama, Aichi 484-8506, ⁴Laboratory of Veterinary Physiology, Tokyo University of Agriculture and Technology, Tokyo 183-8509, ⁵Department of Basic Veterinary Science, The United Graduate School of Veterinary Science, Gifu University, Gifu 501-1193, Japan

Abstract. To determine the effect of *Pueraria mirifica* (PM) on serum parathyroid hormone (PTH) and calcium levels on aged menopausal monkeys (*Macaca fascicularis*), subjects were treated with 10, 100, or 1,000 mg/day of PM. Blood samples were collected every 5 days for 30, 90, and 60 days during pre-treatment, treatment, and post-treatment periods, respectively. Sera were assayed for PTH, estradiol, and calcium levels. PM-1,000 had the strongest effect on the decrease in PTH ($0.001 < P \leq 0.05$) and calcium levels ($0.001 < P \leq 0.03$) during the treatment period. PTH levels remained low for the first 15 days of the post-treatment period ($0.01 \leq P \leq 0.05$). PM-10 induced a significant decrease in PTH level on day 80 ($P = 0.02$) during the treatment period and a significant decrease in calcium level on day 75 ($P < 0.01$). There were no changes in serum PTH and calcium levels throughout the study period in the PM-100 group. Estradiol levels decreased significantly during the treatment period in all treatment groups. The results suggest that long-term treatment with 1,000 mg/day of PM decreases serum PTH and calcium levels in aged menopausal monkeys, indicating that PM ameliorates bone loss caused by estrogen deficiency.

Key words: *Pueraria mirifica*, Phytoestrogen, PTH, Calcium, Aged menopausal monkey

(J. Reprod. Dev. 50: 639–645, 2004)

Menopausal osteoporosis is a disorder of the bone characterized by the progressive loss of bone tissue, and is caused by estrogen deficiency in both natural and surgical menopause [1]. Increased parathyroid hormone (PTH) secretion contributes to an increase in bone resorption and osteoporosis, which is related to estrogen deficiency [2, 3]. Although the exact mechanism has not been elucidated yet, PTH is a major factor involved in

the systemic regulation of bone resorption. Overproduction of PTH leads to an increase in bone resorption compared with bone formation and contributes to general skeletal demineralization. Increased PTH levels have been found to be concomitant with decreased bone mass in aging people [4]. One pathogenetic mechanism of osteoporosis involves chronic loss of calcium balance caused by intestinal and renal calcium handling. This mechanism is characterized by an increase in PTH concentration, and is generally thought to be a secondary response to a small